THz radiation and acoustic phonon pulse wave from GaN-based light emitting diode structures generated by ultra short pulse lasers

Eunsoon Oh,[1]* J.Y. Sohn,[2] J.S. Yahng,[2] Y.D. Jho,[2] D.S. Kim,[2] G.D. Sanders,[3] and C.J. Stanton[3]

[1]Department of Physics, Chungnam National University, Daejeon, South Korea
[2]Department of Physics, Seoul National University, Seoul, South Korea
[3]Department of Physics, University of Florida, Gainsville, FL 32611

ABSTRACT

We discuss the generation mechanism of THz radiation and acoustic phonon pulse wave under ultra short pulse excitations in GaN-based light emitting diode (LED) structures containing InGaN/GaN multiple quantum wells. In order to understand the role of piezoelectricity in the THz radiation and acoustic phonon pulse wave generations, an external field was applied in these structures so that the piezoelectric field in the quantum wells was compensated under an external reverse bias. Coherent acoustic phonon pulse wave was found to be independent of the applied voltage, although the strain of the InGaN layers was crucial for the generation of the signals. The THz emission from these structures was found to increase with increasing reverse voltage and excitation energy, similar to the trend of the photocurrents in these structures. The bias and wavelength dependence of the THz generation suggests the carriers associated with the photocurrents are responsible for the THz radiation.

Keywords: GaN, InGaN, acoustic phonon, strain, THz, piezoelectricity, photocurrent

1. INTRODUCTION

In GaN-based p-i-n junction structures containing InGaN quantum wells, the InGaN layers are highly strained and piezoelectric field is present due to the lack of inversion symmetry in their wurtzite structure [1]. Under the application of a reverse bias, the piezoelectric field is compensated by an external electric field and the strength of the piezoelectric field can be estimated from the shift of the interband transition energy under external bias [2]. Time-domain study using short pulse lasers in GaN-based LED (light emitting diode) structures containing InGaN/GaN multiple quantum wells provides new exciting opportunity to investigate carrier and phonon dynamics under piezoelectric potential associated with the strained InGaN layers.

Phonon frequencies in various materials are commonly studied by cw-Raman measurement. In the Raman process, the wavevector of phonons is given by the change in the wavevector of an excitation laser (wavelength λ in the air), that is, twice of $2\pi n/\lambda$ in the backscattering geometry. The wavevector of the phonons created in this process is close to the zone center of a Brillouin zone since the wavelength of an excitation laser is several orders of magnitude larger than lattice constants.

In multiple quantum wells or superlattice systems, new periodicity corresponding to the sum of the well and the barrier widths is present. Typically, acoustic phonon dispersion curves for the well and barrier materials overlap and acoustic phonons can *propagate* through the entire medium, conserving their frequencies. The propagating acoustic waves with long wavelengths experiencing the new periodicity in the multiple quantum wells make the observation of the zone folded acoustic phonons possible. In cw-Raman measurements, the Raman signals of the folded acoustic phonons appear as doublets. This is in sharp contrast with optical phonons, where the dispersion curves are usually flat, and in many cases optical phonons cannot propagate through the wells and barriers preserving their frequencies. These are called confined optical phonons. In such cases only discrete wavevectors are allowed for the optical phonons, as in standing waves.

Phonon dynamics can be observed in a real time domain by pump-probe experiments. Under ultra short pump pulse excitation, coherent phonons can be generated, i.e., lattices vibrate in phase, resulting in oscillations in refractive index and in oscillations of the reflected or transmitted probe beam intensity. Strong coherent acoustic phonon oscillations

Ultrafast Phenomena in Semiconductors and Nanostructure Materials VIII, edited by Kong-Thon Tsen, Jin-Joo Song, Hongxing Jiang, Proceedings of SPIE Vol. 5352 (SPIE, Bellingham, WA, 2004)
0277-786X/04/$15 · doi: 10.1117/12.531339

associated with folded acoustic phonons in InGaN/GaN multiple quantum wells were observed under short pulse laser excitation [3]. The oscillation period was about 1.4 ps at pump wavelength of 398 nm, expected for folded acoustic phonon frequencies with the longitudinal acoustic phonon velocity of about 7000 m/s. In addition to these folded acoustic phonons, *spatially localized* strain wave traveling with longitudinal acoustic phonon velocity (we now call coherent acoustic phonon pulse wave) was observed. The oscillation period was about 9 ps with excitation wavelength of 380 nm [4].

THz radiation can be generated from optically excited carriers via charge acceleration or via optical rectification. THz emission by charge acceleration can be observed even in the absence of an external field due to built-in field, but the emission can be greatly increased with applied field. It has been known that instantaneous polarization of the electron hole pairs in quantum wells can generate THz radiation. In the presence of an electric field, electrons and holes are spatially separated from each other, creating instantaneous polarization. Time derivative of the polarization corresponds to charge oscillation, or current, creating THz radiation [5]. Weak THz emission from lattice vibration (phonon) corresponding to small acceleration of nuclei has been also reported [6]. Optical rectification or differential frequency mixing originates from the nonlinear interaction between two optical fields, which produces slowly varying electric field at the beat frequency [7].

Sohn et al. observed THz radiation corresponding to 9 ps period from GaN-based LED structures containing InGaN/GaN multiple quantum wells with In concentrations of about 15 % [8]. The THz signal was different from that of a GaN-based double hetero-structure with an InGaN active layer with low In concentration (about 3 %) instead of InGaN/GaN multiple quantum wells. This suggests that the strained InGaN layers are responsible for the THz generation. Since the period of the THz radiation was about 9 ps, the THz radiation appeared to be associated with the acoustic waves.

In this paper, we discuss several issues regarding generation mechanism of the THz radiation observed in GaN-based p-i-n LED structures containing InGaN/GaN multiple quantum wells. In an effort to clarify the role of piezoelectricity in the generation mechanism, reverse bias voltage was applied to these structures and the net electric field in the quantum wells was varied. The bias and wavelength dependence of the THz generation suggests the carriers associated with the photocurrents are responsible for the radiation. We also discuss that the carriers are possibly influenced by the coherent acoustic waves.

2. SAMPLE DESCRIPTION AND EXPERIMENTAL

The GaN p-i-n LED structures were grown on sapphire substrates by metalorganic chemical vapor deposition. The following layers were sequentially grown on undoped GaN: about 4 μ m thick n-GaN, five InGaN/GaN multiple quantum wells with well and barrier widths of 2.2 nm and 10 nm, respectively, 30 nm thick p-AlGaN, and 0.2 μ m thick p-GaN. The In composition was about 15 % for blue LED structures. The Si concentration for n-GaN was about 3×10^{18} cm^{-3}, according to SIMS (secondary ion mass spectroscopy) measurements. The Mg concentrations for p-GaN and p-AlGaN were about 8×10^{19} cm^{-3} and 5×10^{19} cm^{-3}, respectively. As is well known, only small fraction of Mg acceptors are activated due to their large acceptor binding energy, and the hole concentrations for p-GaN and p-AlGaN estimated from Hall measurements were about 2×10^{17} cm^{-3} and 1×10^{17} cm^{-3}, respectively. Typical LED fabrication processes were followed including the transparent p-electrodes with an optical window of 300 μ m x 300 μ m, which allowed optical excitations from the surface. The excitation source was a frequency-doubled Ti:sapphire laser, whose energy was varied between 420 nm to 365 nm for pump-probe experiments and for THz radiation. The pulse width after the frequency doubling was about 250 fs. The peak pump intensity was about 400 MW/ cm^2, corresponding to a carrier density of 10^{19} cm^{-3}. The static breakdown voltage of the LED structures was about - 23 V. All the measurements were carried out at room temperature.

3. RESULTS AND DISCUSSIONS

Figure 1 shows the THz radiation in blue LED structures with InGaN/GaN multiple quantum wells under short pulse excitation of 3.397 eV. In order to understand the role of piezoelectric field in the generation mechanism of acoustic pulse wave and THz emission, external voltage dependence was investigated. As seen in the figure, we observed a

distinct THz radiation of 9 ps period. The period was independent of external bias, but the signal increased with increasing external reverse voltage.

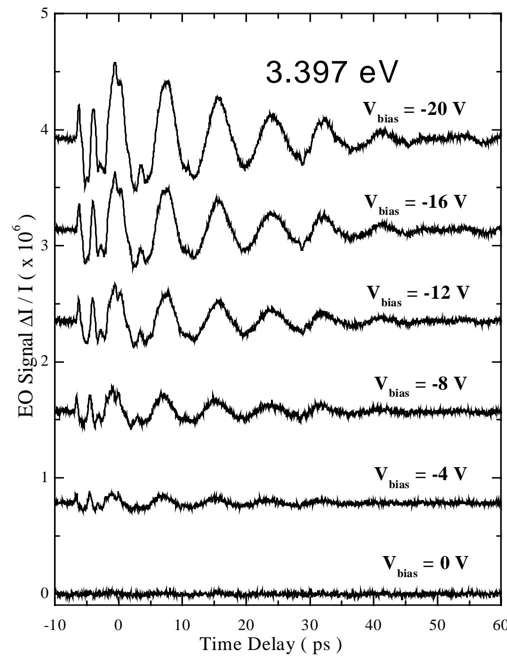

Fig. 1 THz signal from blue LED structures as a function of reverse voltage.

Previous time-resolved photoluminescence study in these structures showed that the electric field present in the strained InGaN quantum wells due to piezoelectricity was compensated in an external field of about 20 V [2]. If the THz radiation were generated by the instantaneous polarization associated with the spatial separation of electrons and holes in the quantum wells, the signal would have decreased with compensating external field. This indicates that the instantaneous polarization is insignificant in THz generation. Moreover, the quantum well width in these structures is too thin to produce enough instantaneous polarization since the well width is of the order of the exciton Bohr radius.

Figure 2 shows the pump-probe data with 3.26 eV from the same structures, where the change of reflectance is plotted as a function of time delay. The rise and fall of the pump-probe signal as a function of delay time indicates the change in refractive index due to the generation and decay of photocarriers. Since the pump and probe energy is near the InGaN bandgap, the rapid decrease of the signal before the time delay of 20 ps with 15 V indicates the rapid decay of the carriers in the InGaN quantum wells. The rapid decay can be well understood as the rapid tunneling of the photocarriers from the InGaN quantum wells through barriers due to the decrease of the effective barrier width with increasing reverse voltage associated with the tilting of the barrier potential.

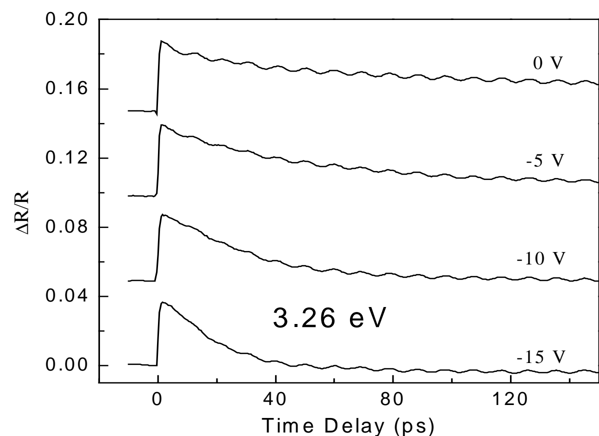

Fig. 2 Differential reflectance as a function of reverse voltage in blue LED structures.

The tilting of the barrier potential energy with reverse bias is schematically shown in Fig. 3. With external voltage, the effective barrier width decreases and tunneling becomes easier. Photocurrents in the LED structures can be both due to the thermionic emission and tunneling currents. Photocurrents were found to increase with increasing excitation energy, which was attributed to the decrease of the tunneling lifetime [2]. Fig. 3(c) shows the energy diagram in a p-n junction under external voltage and shows the increase of the electric field in the depletion region.

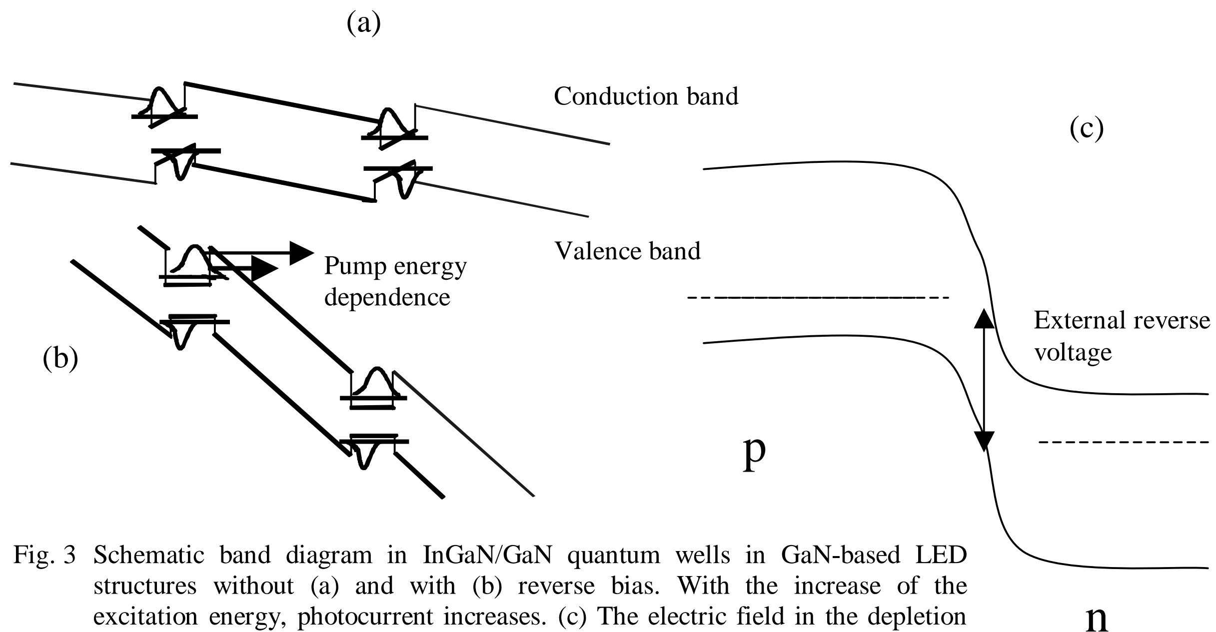

Fig. 3 Schematic band diagram in InGaN/GaN quantum wells in GaN-based LED structures without (a) and with (b) reverse bias. With the increase of the excitation energy, photocurrent increases. (c) The electric field in the depletion region increases with increasing reverse voltage.

As seen in Fig. 2, on top of the background pump-probe signal, there are oscillations of the period of 9 ps. They have been attributed to the interference effect due to the propagation of the strain pulse wave originated from the strained InGaN layers, traversing with longitudinal acoustic phonon velocity. The acoustic pulse wave is a spatially localized square wave, or a wavepacket, rather than typical acoustic wave with a single frequency component observed in Raman scattering.

Figure 4 explains the Fabry-Perot type interference due to acoustic phonon pulse wave. The shaded area corresponds to the strained area, or the intrinsic region of the structures. The tensile strain pulse travels with sound velocity, and the strain pulse modulates the bandgap of GaN. The change of the bandgap produces the local change of the refractive index in the wavepacket. The local decrease of the bandgap due to the strain pulse is estimated to be roughly about 15 meV from the change of refractive index in these structures.

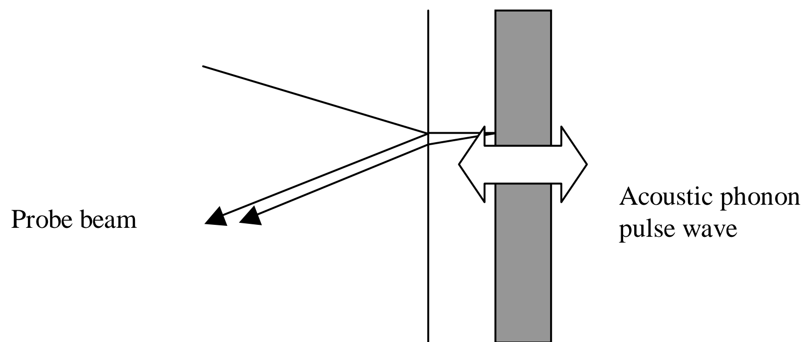

Fig. 4 Interference of the probe beam due to the acoustic phonon pulse wave.

Since GaN is piezoelectric material, the strain pulse can create local electric field. The electric field may affect the absorption by Franz-Keldysh effect and in turn the refractive index. The modulation of the bandgap by strain itself and by Franz-Keldysh effect will now modulate the refractive index as the acoustic pulse wave propagates. Part of the probe beam will be reflected in front of the InGaN layers and part of the beam in front of the wavepacket due to the difference in refractive indices. The two reflected beams interfere constructively or destructively depending on the position of the traveling wavepacket, producing the Fabry-Perot type oscillations in a time domain. Then the oscillation period will correspond to $\lambda/2vn$ since the wavepacket moves with sound acoustic velocity v. Here, λ/n is the wavelength of the *probe* (rather than pump) beam in the medium.

As seen in Fig. 2, the amplitude and period of the oscillations due to the acoustic wave is not much influenced by an external reverse voltage up to 20 V, indicating that the net electric field in the quantum wells is not important for the generation mechanism of the acoustic wave. Under a reverse voltage larger than 10 V, the background pump-probe signal decays at around 30 ps, but the oscillations do not disappear even after the time delay of 30 ps. This indicates that the strain pulse wave propagates even after photocarriers are no longer present in the quantum wells.

Unlike the strain pulse wave, THz radiation is expected only when there remains enough number of carriers that can be accelerated, or oscillated. Here we assume that the radiation due to the acceleration of the atoms is weak and negligible. In order to identify the carriers responsible for the THz radiation, we compare the decay of the THz radiation amplitude as a function of time delay seen in Fig. 1 with the decay of the pump-probe signal in Fig. 2. Note that the decay of the THz radiation seen in Fig. 1 does not resemble the decay of the pump-probe signal with various voltages in Fig. 2. We thus speculate that the carriers creating the THz radiation are not the carriers in the quantum wells.

Figure 5 shows the THz signal as a function of external reverse voltage (squares). We also plotted the photocurrents with excitation energies of 3.31 eV (circles) and 3.12 eV (triangles). The trend of increasing photocurrents with increasing reverse voltage agrees with the increase of THz signals with voltages, except that photocurrent appears to saturate above 4 V, whereas THz radiation keeps increasing with increasing the voltage. We would like to suggest that the carriers responsible for the THz radiation are the carriers associated with photocurrents rather than the carriers in quantum wells. In such case, the THz radiation can last longer than the carrier lifetime measured either by time-resolved photoluminescence or by pump-probe experiments. This explains that the THz radiation can last up to 40 ps (see Fig. 1) regardless of the reverse voltage.

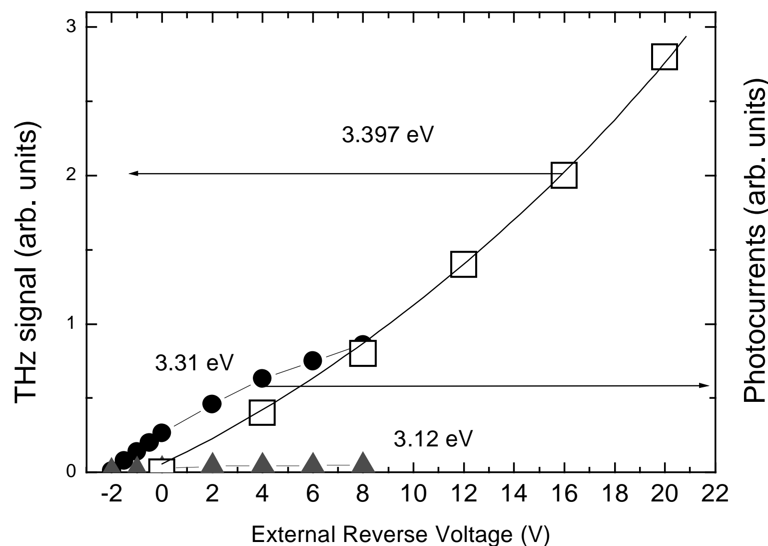

Fig. 5 THz radiation intensity and photocurrents as a function of reverse voltage in the blue LED structures.

The excitation energy dependence of the pump-probe signal and the THz signal at 20 V is given in Fig. 6. Pump-probe signal increases with increasing excitation energy up to 3.3 eV, but decreases above it. The increase below 3.3 eV is mainly due to the increased absorption coefficient and the corresponding increase of photocarriers with increasing excitation energy. Above the photon energy of 3.3 eV, the absorption at the p-GaN layer near the top of the structures rapidly increases and photocarriers *in the quantum wells* begin to decrease. On the other hand, THz signal keeps increasing with increasing excitation energy, *regardless of where the photocarriers are created.* Namely, the photocarriers created in the p-GaN cap layer appear to participate in the THz radiation.

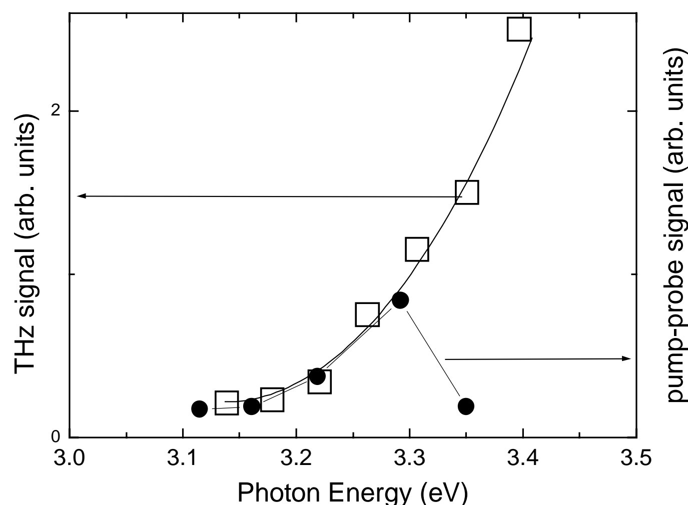

Fig. 6 THz signal and pump-probe signal as a function of excitation energy.

The period of the THz radiation roughly corresponds to the total intrinsic layer thickness of about 60 nm (number of wells, 5, times the sum of the well and barrier widths of 12 nm) divided by the longitudinal acoustic phonon velocity. If longitudinal acoustic phonon of wavelength 60 nm were created, the period of the acoustic wave would be about 9 ps. One possible origin of the THz radiation is the oscillation of carriers due to the electric field associated with the strain pulse wave because of the piezoelectric property of GaN. The oscillation period due to strain pulse wave is about 9 ps, independent of the applied voltage (see Fig. 2). Also in THz radiation, the period is independent of bias.

On the other hand, the oscillation period due to acoustic pulse wave varies with *probe* wavelengths, as expected for any interference effect. The change of the period as a function of probe wavelength is shown in Fig. 7. Also shown with squares is the period of the THz radiation as a function of *pump* wavelength. Unlike the period due to the acoustic pulse wave, that of the THz radiation is independent of the wavelength.

In Fig. 7, it may appear to be contradictory that the period of the acoustic wave is different from that of the THz radiation. As was shown in Fig. 4, the pulse width is determined by the intrinsic layer width, independent of pump wavelength, and the interference pattern depends on the probe wavelength. Both the oscillation period in the pump-probe signal and the THz radiation period are independent of pump wavelength, which is consistent with Fig. 7.

We explained that the carriers responsible for THz radiation are probably the photocarriers that contribute to photocurrents. One remaining question regarding the THz radiation mechanism is whether the carriers are accelerated by the electric field generated by the acoustic pulse wave. The drift velocity of the carriers is generally slow compared to the acoustic phonon velocity. Then the carriers can be considered to be almost steady, while the acoustic phonon pulse wave travels with 7000 m/s. Typically, interaction between carriers and acoustic phonons is rather weak even in

polar materials, but the strain pulse wave may effectively generate local electric field in GaN with the help of piezoelectricity.

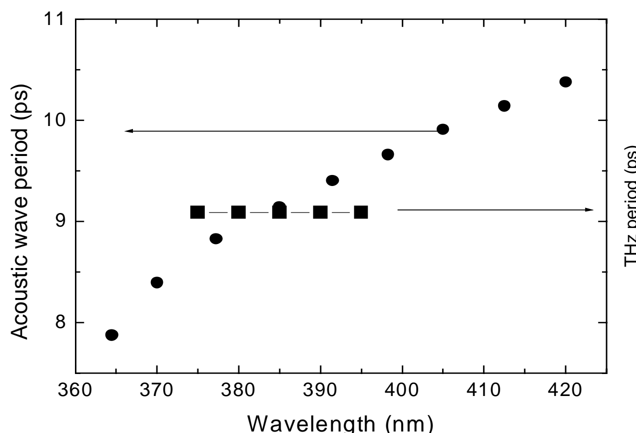

Fig. 7 Oscillation period due to coherent acoustic phonons (circles) as a function of *probe* wavelength and THz radiation period as a function of *pump* wavelength (squares).

4. CONCLUDING REMARKS

We varied the electric field of the InGaN quantum wells in GaN-based LED structures by applying external voltage and investigated the coherent acoustic phonon signal and THz radiation. The duration of the THz radiation was about 40 ps, independent of applied voltage. Since carrier lifetime in the quantum wells drastically decreased with reverse voltages, the carriers responsible for the THz radiation would not be the carriers in the quantum wells.

We suggest that the photocarriers associated with photocurrents are responsible for THz radiation since the THz radiation increases with increasing reverse voltage, similar to the trend of photocurrents. The THz radiation increases with increasing voltage, even though the net electric field in the quantum wells decreases with the reverse voltage, which does not contradict with our model.

Piezoelectricity of GaN appeared to be important both for the propagation of the acoustic strain pulse wave and THz radiation, since the strain pulse can generate electric field in GaN. On the other hand, the net electric field in the quantum wells was not critical in the generation of either the acoustic pulse wave or the THz radiation, which was evident from the external voltage dependence.

In both acoustic pulse wave and THz radiation, the number of photocarriers is important for their generations. In the former, photocarriers have to be generated in the strained quantum wells, but in the latter, photocarriers responsible for photocurrents appear to generate THz radiation.

The period of the acoustic phonon varies with excitation wavelength, whereas that of the THz radiation is independent of the excitation wavelength. This may seem to be contradictory, but one has to bear in mind that the variation of the period in the acoustic phonon signal is due to the *probe* beam rather than due to the *pump* beam. The period of THz radiation is independent of the pump wavelength as in the acoustic phonon pulse wave.

5. ACKNOWLEDGEMENTS

This work was supported by Basic Research Program of the Korea Science & Engineering Foundation (Grant No. R04-2003-000-10020-0).

REFERENCES

1. T. Takeuchi, S. Sota, M. Katsuragawa, M. Komori, H. Takeuchi, H. Amano, and I. Akasaki, Jpn. J. Appl. Phys., Part 2, 36, L382 (1997).
2. Y.D. Jho, J.S. Yang, E. Oh, D.S. Kim, Appl. Phys. Lett. 79, pp. 1130-1132 (2001); Y.D. Jho, J.S. Yang, E. Oh, and D.S. Kim, Phys. Rev. B 66, p. 035334 (2002).
3. C. K. Sun, J.C. Liang, and X.Y. Yu, Phys. Rev. Lett. 84, p. 179 (2000).
4. J.S. Yahng, Y.D. Jho, K.J. Yee, E. Oh, J.C. Woo, D.S. Kim, G.D. Sanders, and C.J. Stanton, Appl. Phys. Lett. 80, pp. 4723-4725 (2002).
5. P.C.M. Planken, M.C. Nuss, W.H. Knox, D.A.B. Miller, and K.W. Goossen, Appl. Phys. Lett. 61, p. 2009 (1992).
6. T. Dekorsy, H. Auer, C. Waschke, H.J. Bakker, H.G. Roskos, H. Kurz, V. Wagner, and P. Grosse, Phys. Rev. Lett. 74, p. 738 (1995).
7. M. Bass, P.A. Franken, J.F. Ward, and G. Weinreich, Phys. Rev. Lett. 9, p. 446 (1962).
8. J.Y. Sohn, J.S. Yahng, D.J. Park, D.S. Kim, E. Oh, J.C. Woo, G.D. Sanders, and C.J. Stanton, 28th Int. Symp. Compound Semiconductors, Tokyo, Japan, p. 387 (2001).

*esoh@cnu.ac.kr; phone 82-42-821-5453; fax 82-42-822-8011